NON LINEAR FINITE ELEMENT ANALYSIS OF REINFORCED AND UNREINFORECED PAVEMENTS

F. Moghadas Nejad

Department of Civil and Environmental Engineering, Amirkabir University of Technology
Hafez Avenue, Tehran, Iran, moghadas@aut.ac.ir

Abstract   In this research a comprehensive finite element program was developed in order to carry out an elasto perfectly plastic analysis of geogrid reinforcement of a model pavement. Qualitative agreement is seen between the numerical results and experiment. The results indicate the influence of geogrid in reduction of vertical deformation of pavements. It is also seen that for strong subgrade, the optimum position of geogrid in base layer is at the level of maximum lateral displacement. This indicates that the main mechanism of geogrid is to restrain soils from lateral displacement through interlocking with the particles. Furthermore, the results show that if deformation of subgrade is concerned (e.g. weak subgrade) the optimum position of geogrid is at the base-subgrade interface due to substantial reduction of horizontal stress transfered subgrade.

Key Words   Geogrid, Reinforced pavement, Finite Element Analysis, Interlocking

چکیده   در این تحقیق یک برنامه جامع المان های محدود غیر خطی بمنظور تحلیل ارتجاعی خمیری روسازی های تقویت شده با ژئوستنتیک ها نوشته شده است. انطباق کیفی قابل قبولی بین نتایج آزمایش و تحلیل مشاهده می‌شود. نتایج آنالیز نشان دهنده تاثیر ژئوگرید در کاهش نشست قائم روسازی است. هم چنین مشاهده می‌شود که در مورد بستر با مقاومت بالا محل بهینه ژئو گرید در لایه اساس و در محل تغییر شکل افقی حداکثر است. نتایج فوق بیانگر این واقعیت است که مکانیسم اصلی عملکرد ژئوگرید جلو گیری از تغییر شکل افقی خاک در اثر قفل شدگی با دانه های خاک بوده و اثر غشای ژئوگرید فقط در نشست های زیاد وارد عمل می‌شود.

1. INTRODUCTION

For many years design of pavements has been based upon experimental methods and experience gained from behavior of previous pavements. However, in recent years the finite element method has increasingly been used for structural analysis of the pavements. The method is especially attractive when the nonlinear behavior of granular and cohesive materials used in pavements is to be considered in mechanistic modeling.

Elastic analyses, which are based on linear behavior, may offer some understanding of pattern of strains and stresses field, however such analyses have limitations. This is because soil behavior cannot usually be described in terms of a linear stress-strain relationship. Thus, many mathematical relationships for the behavior of soil have been developed including models based on non-linear elasto-plastic or elastic models.

The parametric study using a finite element program developed in this study is used to compare the behavior of the reinforced and unreinforced pavements under a single application of a flexible load of radius equal to that of a tire placed on the surface. The calculations are intended to illustrate the stress and displacement fields set up in the pavement by the action of a single passing tire. This ax symmetric model clearly represents a simplification of loading that would occur in practice. However, the model can provide useful qualitative information about the behavior of a reinforced pavement subjected to more complicated loading cases. The analysis is conducted intended for monotonically applied loadings on a reinforced soil layer and is not

applicable to cyclic loading cases. It is intended to use the analysis to identify the effects that reinforcing has on the granular materials.

2. A REVIEW ON PAST RESEARCH

An early parametric study on reinforced pavements described by Zeevaret [1], was based on the use of a large displacement axisymmetric formulation. Interface elements were used to model slip and separation between the reinforcement and the soil. This finite element model was successful in the back-analysis of the results obtained from laboratory scale model tests and for investigating the mechanism of reinforcement.

Poran [2] has described an alternative plane strain finite element model of a reinforced unpaved road. The conclusions of a parametric study carried out using this model included the suggestion that the load spread of distributed in the fill is improved by the presence of the reinforcement.

The use of a large displacement, large strain finite element plane strain model of a reinforced unpaved road to back-analyze a series of physical model tests was described by Burd [3] and Burd and Houlsby [4]. The finite element results were shown to be in good agreement with the experimental data. For the particular material properties used in the study, however, the finite element results gave no indication that the presence of the reinforcement significantly modified the load-spread behavior of the fill.

Burd and Brocklehurst [5] carried out a small displacement finite element parametric study in order to investigate the mechanism of reinforcement in a plane strain model of reinforced unpaved road under the action of a single monotonic load for small rut depth which is common in paved roads. The results of this study, in which reinforcement stiffness was the variable parameter, indicated that for the design of unpaved roads with small rut depths, it is necessary to choose a geotextile having a stiffness that is sufficient to provide a satisfactory increase in load bearing capacity. The study suggested that, for static loading, there is a little benefit to be gained from using excessively stiff reinforcement. In

the case of very stiff reinforcement, large shear stresses are induced between the soil and the reinforcement which gives rise to large values of reinforcement force.

As it is clear in the above-mentioned works, plane strain formulation has been utilized to analyze reinforced roads. For unpaved roads where large deformation or rutting is acceptable (up to 75mm) plane strain analysis can be a realistic approach to the problem. However, in low deformation systems such as paved roads, axisymmetric formulation may present a more sophisticated approach of stress and strain analysis of the system.

Hence, in this paper an elasto-plastic axisymmetric formulation is presented to analyze reinforced pavements. A one-quarter scaled down geogrid reinforced model pavement constructed in Center for Geotechnical Research at The University of Sydney is used and the results are compared with the experimental records.

3. FINITE ELEMENT FORMULATION

3.1 General Aspect A comprehensive nonlinear axisymmetric finite element program was developed in this research. Analysis carried out using an elastic-perfectly plastic model for the soil, an elastic-perfectly plastic model for the interface element and non-linear model for the geogrid. The results of a model pavement analysis are presented and a comparison is made between the numerical and the experimental results of the model pavement.

3.2 Soil Element The wearing course, base and subgrade were modeled using eight- nodded isoperimetric elements. As the base and subgrade layers used in the modeled pavement were cohesion less materials (c = 0) they were assumed to obey Matsuka failure criteria, Equation 1 [6], and have a non-associated flow rule.

$$f = \frac{I_1 I_2}{I_3} - K_{MN} \tag{1}$$

where:

$$K_{MN} = \frac{9 - \sin^2 \phi'_c}{1 - \sin^2 \phi'_c} \tag{2}$$

$$I_1 = \sigma_1 + \sigma_2 + \sigma_3 \tag{3}$$

$$I_2 = \sigma_1\sigma_2 + \sigma_2\sigma_3 + \sigma_3\sigma_1$$

$$I_3 = \sigma_1\sigma_2\sigma_3$$

ϕ'_c = friction angle measured in triaxial compression

The wearing course was assumed to be elastic material.

3.3 Reinforcement Model   Because the relation between strain and stress in geosynthetics is nonlinear and the tangent moduli decrease significantly as strain increases, making it very inaccurate to use the initial modulus for any strain other than zero, some researchers [e.g. 7,8,9] have proposed mathematical models to provide an efficient means of obtaining the tangent moduli at any point on the stress-strain curve between the origin and the yield peak. In most cases the models for the moduli are n-order polynomials.

Generally strain-stress relations for geosynthetic materials obtained from a uniaxial test, is available from the manufacturer. In the present finite element program, a subroutine based on the least square method was developed to fit the best curve to experimental results. Thus, it is only necessary to give a few points from an experimental load-strain test as input to the program, and the coefficients in the best-fit polynomial can be found.

A general load-strain relationship for a geosynthetic material can be given by:

$$T = A.\sigma = a_1.\varepsilon + a_2.\varepsilon^2 + a_3.\varepsilon^3 + \ldots\ldots\ldots + a_n\varepsilon^n \tag{4}$$

where:

T	axial load
A	initial cross sectional area
$a_1, a_2, a_3\ldots$	Polynomial constants

Differentiation of Equation 4, gives the instantaneous tangent modulus as:

$$\frac{dT}{d\varepsilon} = \frac{d(A.\sigma)}{d\varepsilon} = \frac{Ad\sigma}{d\varepsilon} = A.E_T$$
$$= a_1 + 2a_2.\varepsilon + 3a_3.\varepsilon^2 + \ldots + na_n\varepsilon^{n-1} \tag{5}$$

where:

E_t tangent modulus

a_1, a_2, a_3, **...,** a_n are determined by the least squares fitting technique.

In the case of the geogrid used in this study (Tensar SS2), the result of a uniaxial test on a sample has been presented in Tensar's product catalogues. The load-strain equation for Tensar SS2 (using the curve of best fit which is a polynomial of order 5 (n = 5) and R squared of 0.997 was found to be:

$$T = (3.5350)\varepsilon - (0.1134)\varepsilon^2 + (0.7417E - 01)\varepsilon^3 - (0.1462E - 01)\varepsilon^4 + (0.7320E - 03)\varepsilon^5 \tag{6}$$

where force T is kN/m and ε is in %.

Differentiation of Equation 6 gives the tangent modulus of Tensar SS2

$$\frac{dT}{d\varepsilon} = A.E_T = (3.5350) - (0.2268)\varepsilon + (0.2225)\varepsilon^2 - (0.5848E-01)\varepsilon^3 + (0.3660E-02)\varepsilon^4 \tag{7}$$

where:

$A = (1 \times t)$	initial cross section of a strip per meter length (m^2)
t	thickness (m)
E_T	(kN/m^2)

The reinforcement is considered to have negligible compressive strength. Thus, if during the analysis any compressive stress is detected at a Gauss point, the program attributes a very small elastic modulus to that particular Gauss point and the stiffness matrix is assembled again.

3.4 Interface Element In order to model the interaction and relative displacement between the soil and the reinforcement it is necessary to include an interface element. The interface element consisted of a pair of dual nodes occupying the same position with independent shear and axial stiffness.

Specifying high stiffness until the stress state in the joint reaches the Mohr-Coulomb's failure surface ensures compatible displacement between the pair of dual nodes in an interface element. Once the interface shear strength is exceeded, the joint is allowed to behave as a plastic material.

Some researchers like authors of Reference 10 have appreciated the importance of considering the restraining effect of geogrids in reinforced soil structures. To satisfy this fact in modeling interaction between the geogrid and soils, dilatancy of the soil-geogrid interface and also of the soil itself are taken into account in the analysis.

For an elastic joint (interface) element, the relationship between the force per unit length in the joint and the relative displacement of the element nodes is given by

$$\begin{bmatrix} P_s \\ P_n \end{bmatrix} = \begin{bmatrix} k_s & 0 \\ 0 & k_n \end{bmatrix} \begin{bmatrix} w_s \\ w_n \end{bmatrix} \tag{8}$$

where:

P_s, P_n = shear and normal forces per unit length, respectively.
w_s, w_n = shear and normal relative displacement of the element nodes.
k_s, k_n = joint stiffness in the shear and normal directions.
Once the joint is plastic we can write

$$\begin{bmatrix} \Delta P_s \\ \Delta P_n \end{bmatrix} = \frac{k_s k_n}{\Lambda} \begin{bmatrix} \tan\phi.\tan\psi & \pm\tan\phi \\ \pm\tan\psi & 1 \end{bmatrix} \begin{bmatrix} \Delta w_s \\ \Delta w_n \end{bmatrix} \tag{9}$$

where:

$$\Lambda = k_s + k_n \tan\phi \tan\psi$$

In deriving Equation 9 it has been assumed that the interface dilates at an angle ψ and that it behaves according to the Mohr-Coulomb failure criterion.

$$|P_s| = P_n \tan\phi + C \tag{10}$$

where:

C = the cohesive force per unit length in the joint

The ± signs in Equation 9 arise because of the fact that the shear stress can be positive or negative at failure.

The properties selected for interface elements are presented in Table 2.

4.4 Updating the Mesh The membrane effect is a mechanism of reinforcement behavior, which can be significant when the soil undergoes large deformation. Thus, once deformation has become large this mechanism should be taken into account. To make this possible during the analysis of a problem depending upon the size of load step and rate of deformation, the program can update the mesh every few load steps using:

$$x_i^{(n)} = x_i^{(n-1)} + \delta u_i^{(n)} \qquad i = 1, 2, 3 \tag{11}$$

$$y_i^{(n)} = y_i^{(n-1)} + \delta w_i^{(n)}$$

where:

x, y coordinates of node

u, w   displacements of node in x, y directions, respectively

i No. of node

n No. of load step

This is not a true large strain formulation, as the rotation of stresses is not taken into account in the solid elements, however the rotation of the reinforcement is important, as the membrane effect depends on this.
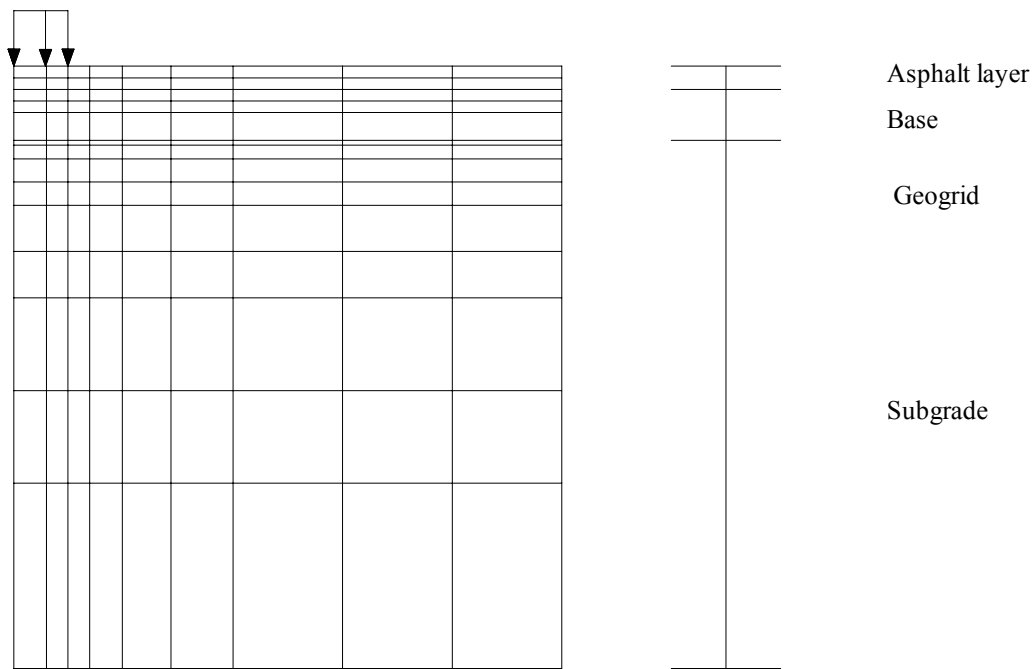
Figure 1. Mesh for pavement.

4. ANALYSES OF MODEL PAVEMENT

In this section, the results of the elasto-plastic analyses performed on the model pavement are presented and a comparison is made between these results and the road machine test results [11].

4.1 Finite Element Mesh   According to the model pavement, the thicknesses of wearing course layer, Base layer and subgrade were considered to be 20, 50 and 500 mm, respectively.

The finite element mesh for each of the analyses consist of 144 elements and were divided into 3 element groups. These element groups were used to represent the soil, the geogrid and the interfaces between the soil and geogrid. Each of the interface element groups consisted of eighteen six-noded isoparametric interface elements with zero thickness and were placed between the soil elements and the reinforcement elements. Nine 3-node isoparametric bar elements were included as an element group

to model the behavior of the geogrid reinforcement (Figure 1).

4.2 Material Properties   Two elastic parameters, namely the Young's modulus (E) and Poisson's ratio (μ), were selected on the basis of published data on pavement materials. Brown and Barksdale [12] suggested an E value of 100 MPa for good materials. To allow for different compaction methods and material types, the base of the model pavement was assumed to have an E value of 75 MPa in this study.

The modular ratio between the road base and the subgrade is usually taken to be 1.5 to 5.0 as recommended by Pell [13] and a ratio of 1.5 was selected for the pavement analysis here, which gave an E value of 50 MPa for the subgrade.

As suggested by Brown and Pell [14], the Poisson's ratios for both the base and subgrade material were chosen to be 0.3.

Unfortunately, the manufacturer provides no information about the properties of the wearing course material and in any case this would be

TABLE 1. Physical Properties of Soils [15].

	Angle of dilation (Ψ)[a] (deg.)	Angle of friction (ϕ)[b] (deg.)
Base material (5 mm aggregate)	15.3	50.7
Subgrade material (sand)	7.3	42.3

Note:

[a] From large shear box test
[b] From triaxial test

TABLE 2. Properties of Interfaces [15].

	Angle of dilation (Ψ)[a] (deg.)	Angle of friction (ϕ)[b] (deg.)	Shear stiffness (kN/m³/mm)	Normal stiffness (kN/m³/mm)
Base-geogrid interface	14.3	73.5	10^7	10^7
Subgrade-geogrid interface	8.3	55.5	10^8	10^8

Note:

[a] From large shear box test
[b] From pull out test

temperature dependent. However, since its maximum particle size is equal to that of the base material and because it has a bituminous binder, it probably has an elastic modulus that is higher than that of the base layer material. For this reason the values of E and μ of this material were selected to be 100 MPa and 0.3, respectively.

As was mentioned previously the Matsuoka model was used as the failure criterion. Because the friction angle used in this model is obtained from triaxial tests, conventional static triaxial tests were conducted on both soils to estimate the friction angle of the two soils, Table 1 [15].

Even though the experimental test results (i.e. road machine test) showed no relative displacement between the geogrid and the soil, provision was made in the program to allow potential relative displacement of the geogrid and the soil. Therefore, in order to investigate the behavior of the soil-geogrid interface it was decided to include interface elements in the analysis.

As mentioned, the experimental results showed that no relative displacement was to be expected and hence high shear stiffness and normal stiffness were selected for the soil-geogrid interfaces. (Table 2).

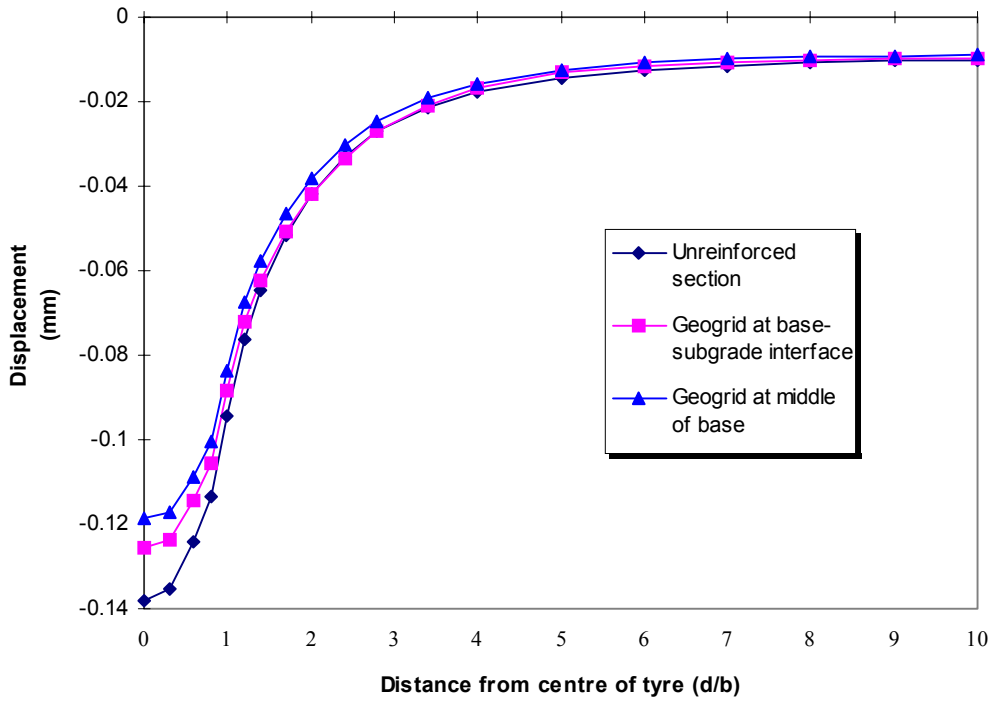**Elasto-plastic finite element analysis of pavement**

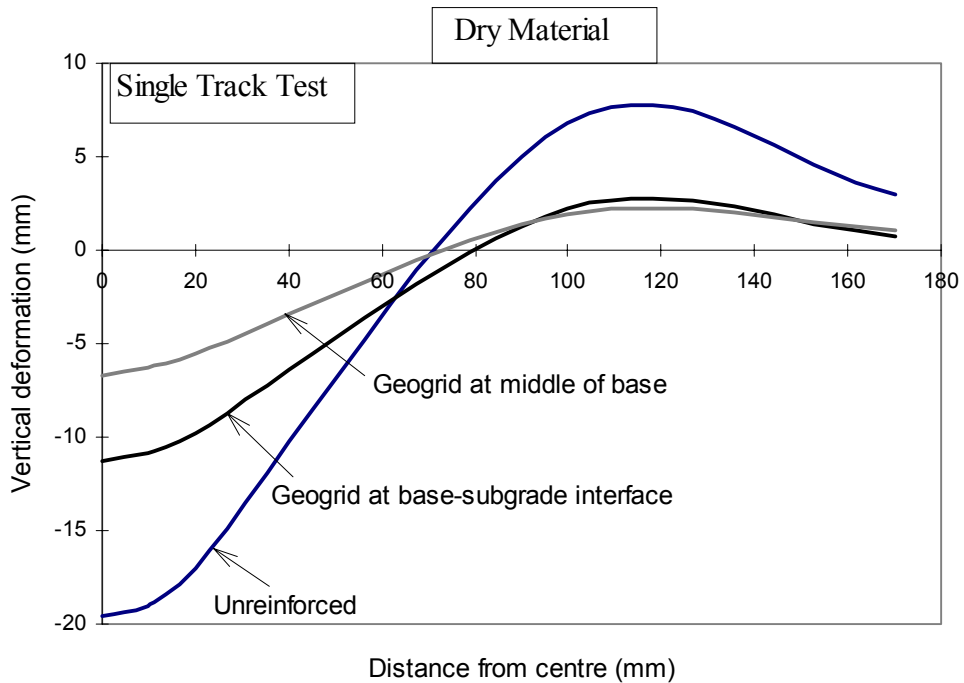**Figure 2.** Vertical deformation of surface (numerical results).

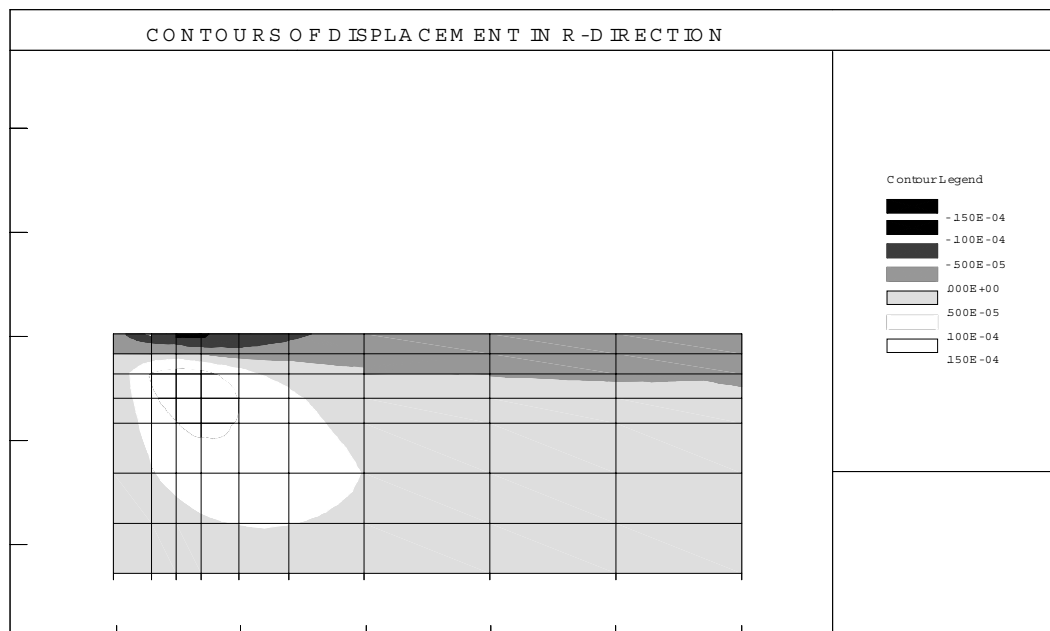**Figure 3.** Vertical deformation of surface at pass No. 3700 experimental test results) [15].

Figure 4. Unreinforced pavement.

To measure the interface properties (i.e. the friction angle and dilatancy angle) a comprehensive set of large shear box tests and pull out tests were conducted on the geogrid [15].

The apparent friction angle measured from pull out tests was selected for the interfaces. However, because the dilatancy angle of the interfaces was not available from the pullout tests, those measured from the shear box tests were chosen as the dilatancy angle of the interfaces (Table 1).

Furthermore, the results of large shear box tests conducted on the two pavement soils without any geogrid [15] showed that $\phi \neq \psi$, which indicates that the two materials have non associated flow rules. Therefore, both soils were assumed to have a non-associated flow rule. The dilatancy angles of the two soils obtained from the shear box test results are presented in Table 2.

The stress dependent elastic modulus of the geogrid, as already mentioned, was obtained from Equation7 by using the curve of best fit to the uniaxial test result for the geogrid provided by the manufacturer.

4.2 Representation of Wheel Loading The tire loading was assumed to be uniform and acting normal to the pavement surface, so that there was no shear stress applied over the contact area.

The tire load was 165 kPa that is equal to the load used in the road machine tests, and this was applied over a circular area of 50 mm diameter [15].

5. RESULTS AND DISCUSSION

Overall displacement of the surface of the pavement as computed from the program is plotted in Figure 2. As may be seen, reduction in vertical displacement due to the presence of the geogrid at the middle of the base (GMB) is higher than that with geogrid at the base-subgrade interface (GBSI). This result is qualitatively in agreement with experimental test results Figure 3.
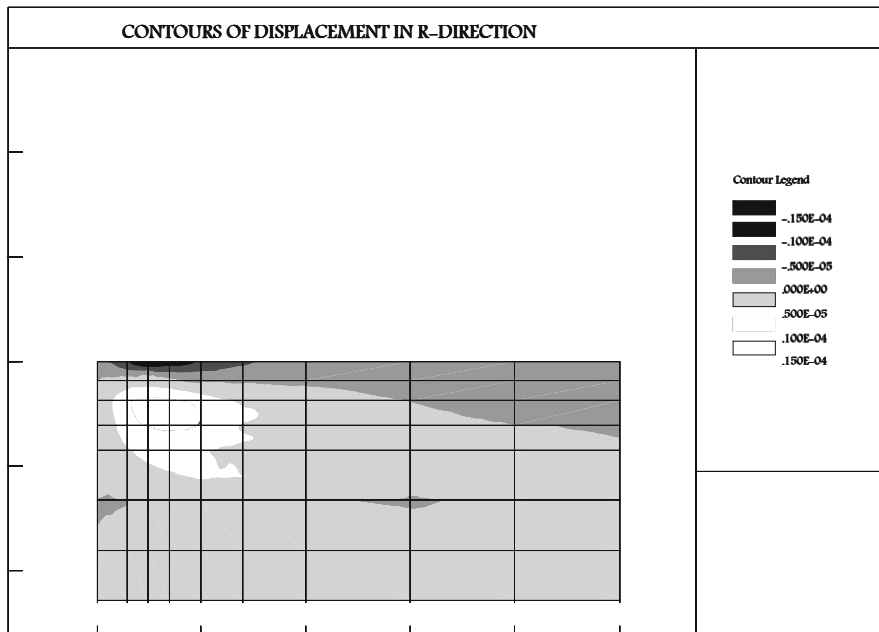
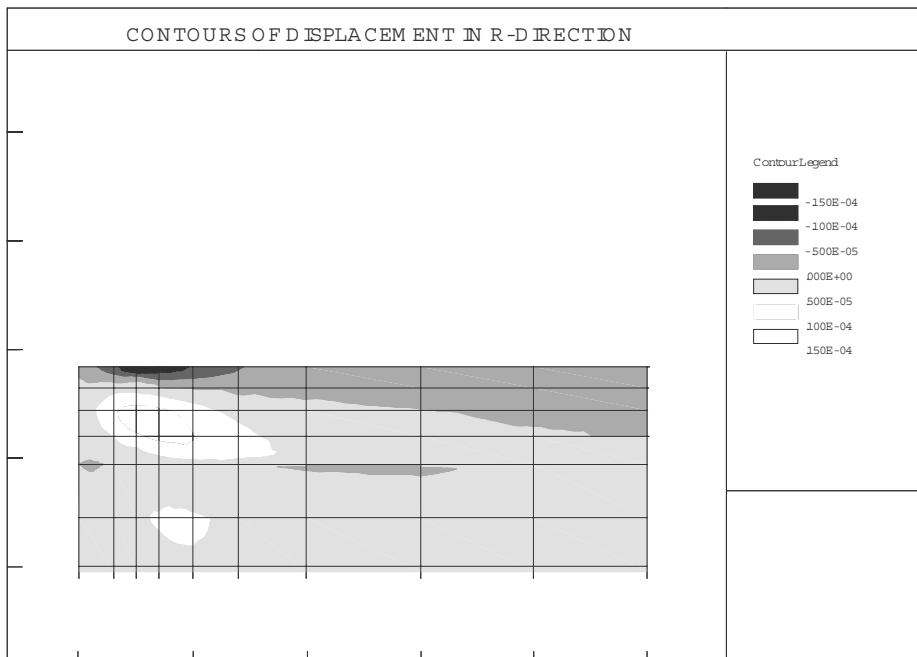**Figure 5.** Geogrid at base-subgrade interface.

Figure 6. Geogrid at middle of base.

Figure 4 shows the lateral movement of the pavement layers in the region beneath the wheel. The lateral displacement near the middle of the base is higher than at the bottom. Thus, if a geogrid is placed at the middle of the base, it should be expected to be more effective in decreasing the lateral displacement. Figures 5 and 6 show the contours of lateral displacement in the pavement

**Radial stress with depth
Elasto-Plastic Finite Element
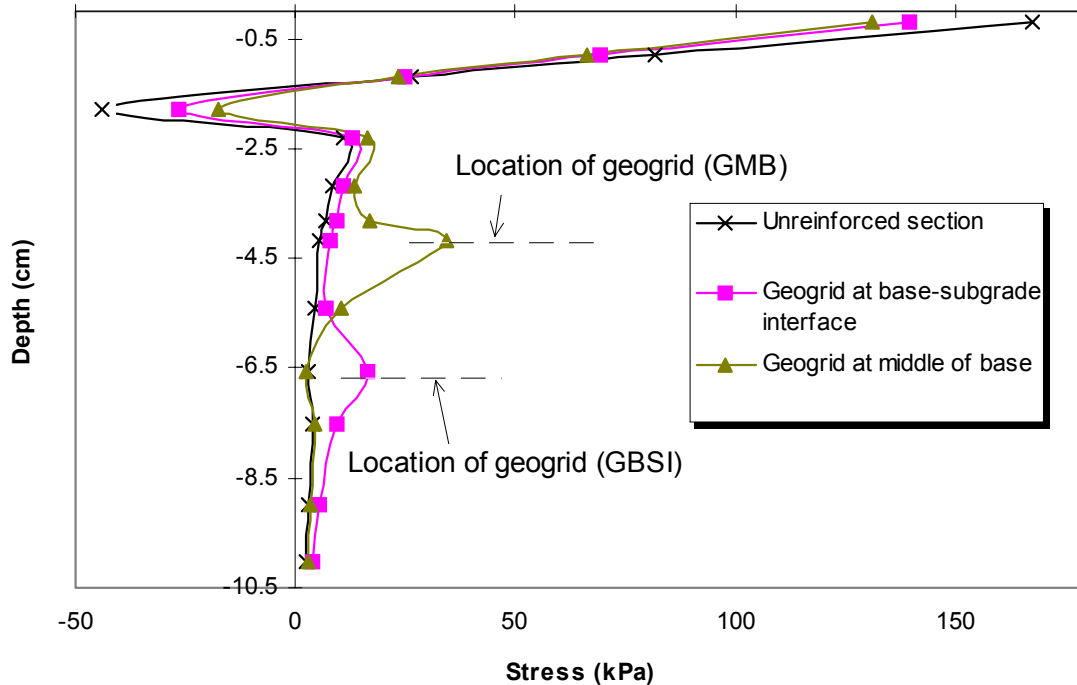Analysis of the Pavement**

Figure 7. Radial stress with depth along the centerline.

for the GBSI and GMB cases, respectively. More significant improvement in reducing lateral movement of the soil in the GMB case is obvious.

These results show that in pavements where displacements are small, the main function of the geogrid is interlocking with the soil particles, preventing lateral movement of the soil.

Figure 7 shows the radial stress within the pavement layers with depth along the centerline. It may be seen that in the region adjacent to the reinforcement, stresses increase significantly. This suggests that lateral restraint imposed on the material by the presence of the geogrid is increasing the stress laterally. The increase of shear stresses adjacent to the reinforcing for the GMB case is higher than that for the GBSI case that indicates that the membrane at the middle of the base layer has been more effective. The other

result that can be noted from this figure is that high tensile stresses exist at the bottom of the wearing course in all cases. However, in the reinforced section the magnitude of this stress has reduced. For the GMB case this reduction is higher. The reason is that according to the theory of elasticity, tensile stress at the bottom of the wearing course is reduced by decreasing the ratio of the elastic moduli of the wearing course and the soil below, (E_w/E_s). This is an indication that the stiffness of the soil has been increased due to the presence of the geogrid.

These results also indicate that a geogrid can be effective in reducing fatigue cracking due to tensile stresses at the bottom of the wearing course.

Figure 8 shows the stress within the geogrid. It may be observed from the figure that for the GMB case there is a higher tensile stress in the

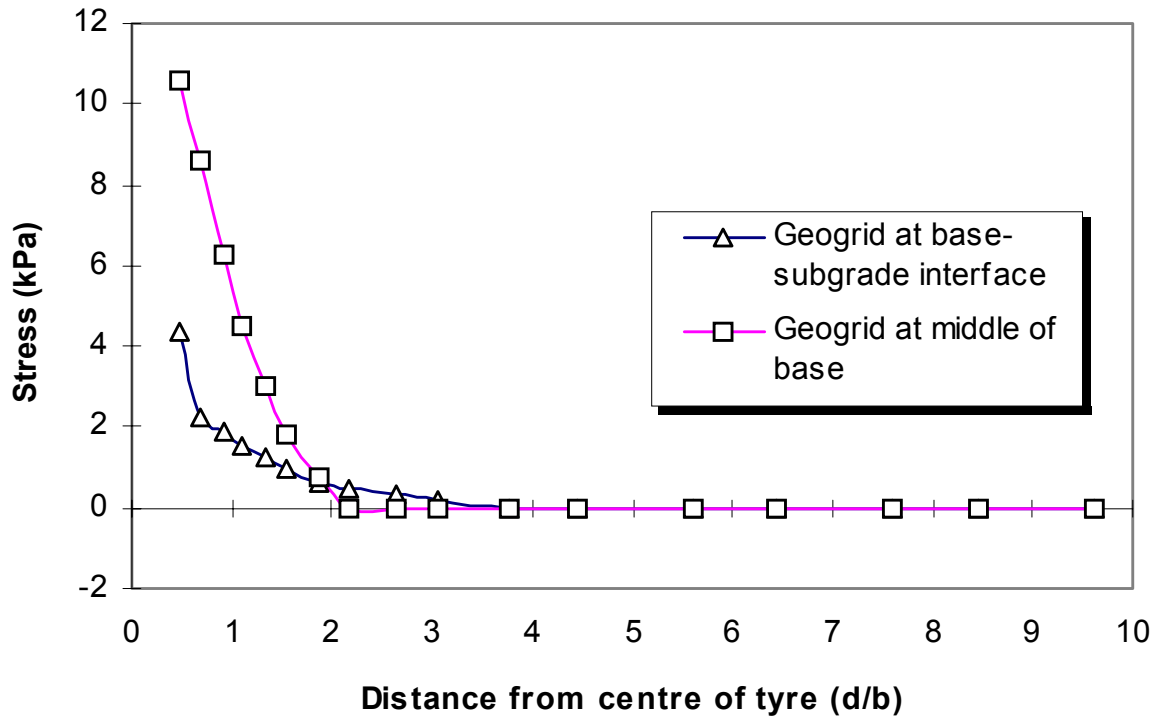## Stress within geogrid
Elsto-plastic analysis of pavement

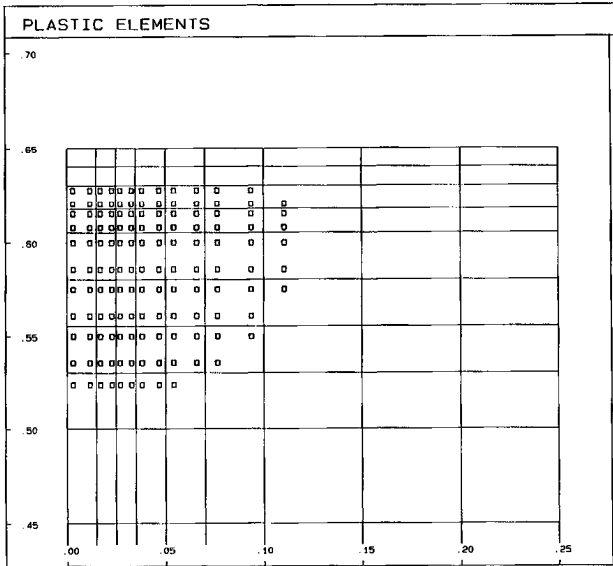**Figure 8.** Stress within the geogrid.

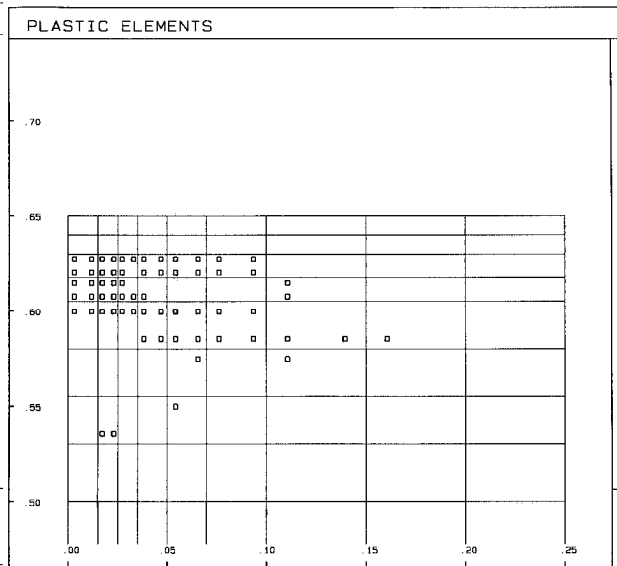**Figure 9**. Unreiforced pavement.

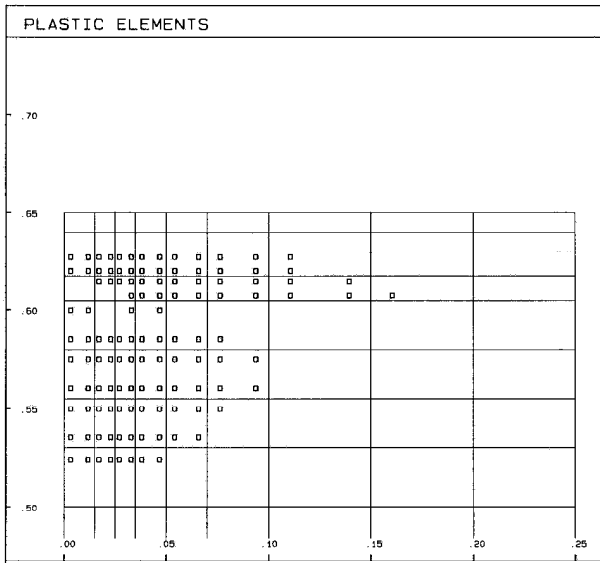**Figure 10**. Geogrid at base-subgrade interface.

Figure 11. Geogrid at middle of base.

membrane than for the GBSI case which confirms the result from Figure 6. It shows that the geogrid at the middle of the base has been more effective in reduction of shear stresses transmitted to the soil below.

Furthermore, this figure can be used as an indication of the minimum required anchorage length of the geogrid. For the GMB case, the length is of the order of 2B while for the GBSI case it is about 4B. This can be explained by looking at Figure 4. Even though for the GMB case, the maximum lateral movement adjacent to the geogrid is more, the rate of decrease of displacement with distance from the center of the load is higher than for the GBSI case.

Figures 9, 10 and 11 illustrate the extent of predicted plastic failure zone within the pavement at the same load (165 kPa). It can be observed from the figures, that there is a reduction in the number of plastic elements immediately beneath the geogrid. The reason is that the geogrid reduces the shear stress transmitted to the soil below it and as a result increases the bearing capacity of the soil. As can be seen, more plastic elements are within the base above the geogrid indicating higher shear stress in this region and consequently the GMB being more involved.

Figure 12 shows the variations of vertical deformation with depth and Figure 13 shows vertical deformation of the surface of the subgrade, respectively. Even though the overall displacement of the surface of the pavement for the GMS case is less than that for the GBSI case, the vertical displacement at the subgrade surface for the GBSI case is less than for the GMB case. This is also what was observed in the road machine test result [11]. The reason is that the geogrid at the base-subgrade interface has been effective in reduction of the shear stress transmitted to the subgrade. This is confirmed by Figures [10,11]. If we look again at these figures it can be observed that the number of plastic elements within the subgrade for the GBSI case is less which means that the shear stress transmitted to the subgrade was less than for the GMB case. Thus, as far as improving the bearing capacity of the subgrade is concerned, the geogrid at the bottom of the base layer was more desirable.

The results of finite element analyses show that a large proportion of vertical and lateral deformation Figures 12 and 14 occur in the base layer. This confirmed the results of an earlier finite element study of pavements carried out by Duncan et al. [16], which mentioned that if the stiffness of the asphalt material is low, the granular material exhibits a very low modulus under the loaded area and a large proportion of the surface deflection can be attributed to deformation within this material.

6. SUMMARY AND CONCLUSION

- The main mechanism of a geogrid in low deformation systems is to restrain soils from lateral displacement through interlocking with the particles. A substantial reduction in horizontal stress transmitted to the soil below occurs because of the presence of the geogrid and consequently the bearing capacity of the soil is increased.
- A geogrid is effective in the reduction of tensile stress at the bottom of the wearing course, which is the main cause of fatigue cracking in a pavement. This results in increasing the life of a pavement.
- The finite element technique can be used in understanding the basic behavior of reinforced
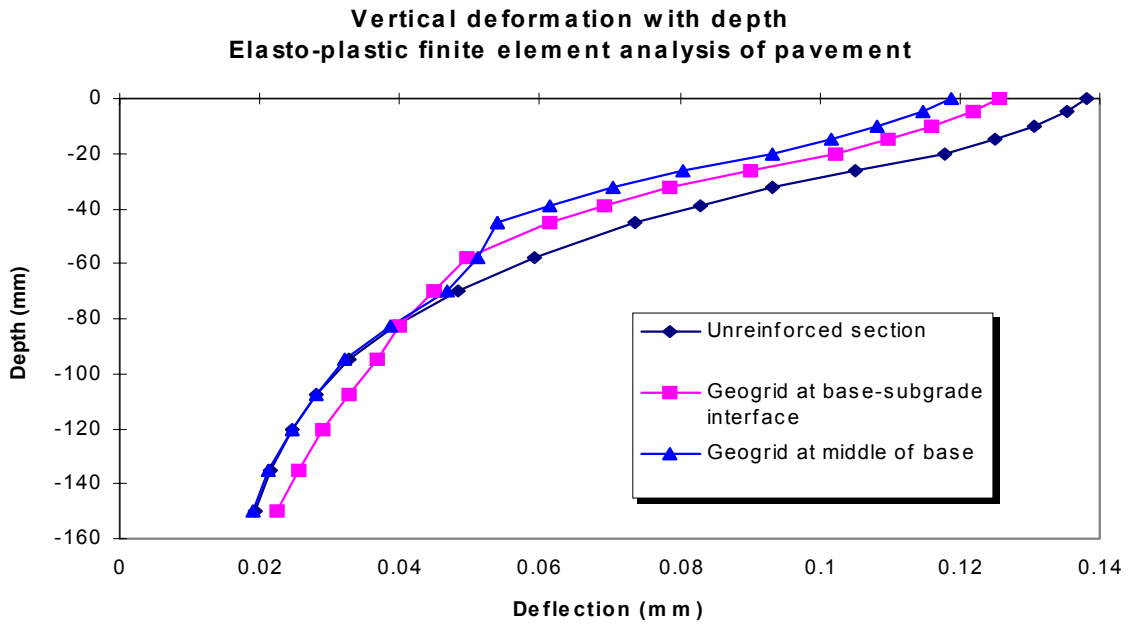
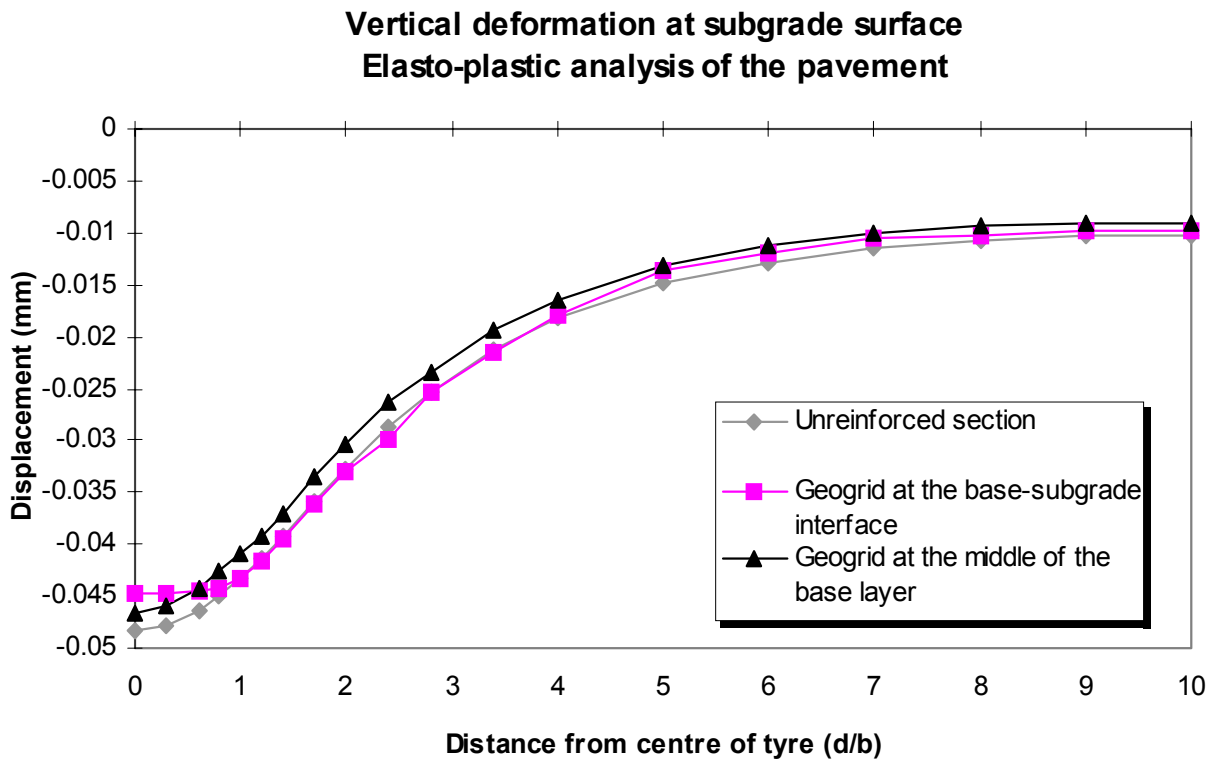**Figure 12.** Vertical deformation with depth.

Figure 13. Vertical deformation of the subgrade surface.

and unreinforced soil systems. To obtain such information experimentally is much more difficult.

- The finite element method may be used in determining the optimum position of reinforcement within the pavement layers to gain maximum efficiency (in terms of surface displacement).

- If the stiffness of the asphalt material is low, the granular material exhibits a very low modulus under the loaded area and a large proportion of the surface deflection can be attributed to deformation within this material.

7. REFERENCES

1. Zeevaert, A. E., "Finite Element Formulation of the Analysis of Interfaces, Nonlinear and Large Displacement Problems in Geotechnical Engineering", Ph.D. Thesis, Georgia Institute of Technology, Atlanta, GA, (1980).
2. Poran, C. J., "Bearing Capacity of Geogrid-Reinforced Granular-Base Overlaying Soft Clay", Ph.D. Thesis, University of California, Davis, USA, (1985).
3. Burd, H. J. A., "Large Displacement Finite Element Analysis of a Reinforced Unpaved Road", D. Phil. Thesis, University of Oxford, U. K. (1986).
4. Burd, H. J. and Houlsby, G. T., "Numerical Modelling of Reinforced Unpaved Roads", *Third Int. Symp. on Numerical Models in Geomechanics*, Canada, (1989), 699-706.
5. Burd, H. J. and Brocklehurst, C. J., "Finite Element Studies of the Mechanics of Reinforced Unpaved Roads", *Proc. of the 4th Int. Conf. on Geotextiles, Geomembranes and Related Products, Rotterdam*, Vol. 1, (1990), 217-221.
6. Matsuoka, H. and Nakai, T., "Stress-Deformation and Strength Characteristics of Soil Under Three Different Principal Stresses, Soils and Foundations", *Proc. Japanese Society of Civil Engineering*, Vol. 232, (1974), 59-70.
7. Giroud, J. P., "Analysis of Stresses and Elongations in Geomembranes", *Proc. of the Int. Conf. on Geomembranes, Denver, USA*, Vol. 2, (1984), 481-486.
8. Giroud, J. P., "Mathematical Model of Geomembrane Stress-Strain Curves with a Yield Peak", *Geotextiles and Geomembranes*, Vol. 13, (1994), 1-22.
9. Giroud, J. P., Monroe, M. and Charron, R. M., "Strain Measurement in HDPE Geomembrane Tensile Tests", *Geotech. Testing J.*, ASTM, Vol. 17, No. 2, (1994), 65-71.
10. Otani, J., Ochiai, H. and Hatashi, S., "Restraining Effect of Geogrid Reinforced Soil in Finite Element Analysis", *Earth Reinforcement Practice*, Balkema, Rotterdam, (1992), 147-150.
11. Mogaddas-Nejad, F. and Small, J. C., "Effect of Geogrid Reinforcement in Model Track Tests on Pavements", *Journal of Transportation Engineering Div.*, ASCE, Paper No. 11952, Vol. 122, (1996), No. 6.
12. Brown, S. F. and Barksdale, R. D., "Pavement Design and Materials", *Proc. 6th Int. Conf. on Struc. Design of Asphalt Pavements, Ann Arbor*, Vol. 2, (1987), 117-148.
13. Pell, P. S., "Pavement Materials", *Proc. 6th Int. Conf. on Struct. Design of Asphalt Pavements, Ann Arbor*, Vol. 2, (1987), 35-70.
14. Brown, S. F. and Pell, P. S., "A Fundamental Structural Design Procedure for Flexible Pavements", *Proc. 3rd Int. Conf. on Struct. Design and Analysis of Sand Masses,* London, (1972), 369-381.
15. Moghadas-Nejad, F., "Geogrid Reinforcement of Pavement", Ph.D. Thesis, The University of Sydney, Australia, (1996).
16. Duncan, J. M., Monismith, C. L. and Wilson, E. L., "Finite Element Analysis of Pavements", *Highway Research Record*, No. 228, (1968), 18-31.